Inorganic Chemistry
Cite This: Inorg. Chem. XXXX, XXX, XXX−XXX
Article
pubs.acs.org/IC

# Octadentate Oxine-Armed Bispidine Ligand for Radiopharmaceutical Chemistry

Neha Choudhary,[†,‡] Alexander Dimmling,[†,§] Xiaozhu Wang,[†] Lily Southcott,[†,‡] Valery Radchenko,[‡,∥] Brian O. Patrick,[∥] Peter Comba,*[,§] and Chris Orvig*[,†]

[†]Medicinal Inorganic Chemistry Group, Department of Chemistry, University of British Columbia, 2036 Main Mall, Vancouver, British Columbia V6T 1Z1, Canada

[‡]Life Sciences Division, TRIUMF, 4004 Wesbrook Mall, Vancouver, British Columbia V6T 2A3, Canada

[§]Anorganisch-Chemisches Institut and Interdisciplinary Center for Scientific Computing, Universität Heidelberg, INF 270, D-69120 Heidelberg, Germany

[∥]Department of Chemistry, University of British Columbia, 2036 Main Mall, Vancouver, British Columbia V6T 1Z1, Canada

Supporting Information

**ABSTRACT:** In this study, we present the synthesis and characterization of the octadentate bispidine ligand, $H_2$bispox$^2$ and its complexes with medicinally useful radiometal nuclides ($^{111}In^{3+}$ and $^{177}Lu^{3+}$), including their X-ray diffraction single crystal structures with the stable isotopes. $^{111}InCl_3$ radiolabels the ligand quantitatively at ambient conditions ([L] = $10^{-5}$ M, room temperature, pH 7 and 15 min) and the in vitro human serum stability assays demonstrated high stability of the $[^{111}In(bispox^2)]^+$ complex over 5 days. Moreover, the $\beta^-$ emitter $^{177}Lu$ radiolabels the ligand at 37 °C in 30 min (pH 8). These initial investigations reveal the potential of the octadentate bispidine ligand $H_2$bispox$^2$ as a useful chelator for $^{111}In$ and $^{177}Lu$-based radiopharmaceuticals.

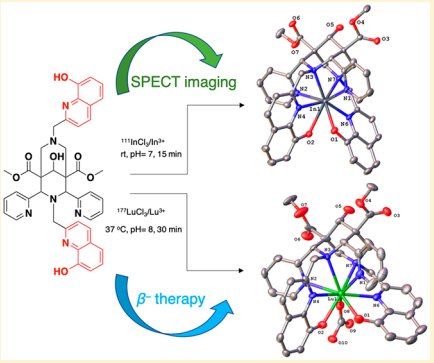


## INTRODUCTION

Since the first clinical study in 1925 using bismuth-214 as a radiotracer to measure blood flow from arm to opposite arm,[1,2] the increasingly diverse use of radionuclides has been expanding the field of nuclear medicine, both in terms of diagnostic imaging (e.g., single photon emission computed tomography, SPECT, and positron emission tomography, PET) and targeted therapy (e.g., alpha ($\alpha$), beta ($\beta^-$), and Auger electron-therapy).[3] A wide range of metallic radionuclides with varying physical (e.g., half-life, specific activity, emission type) and chemical (e.g., hardness, acidity) properties can be produced by cyclotrons, nuclear reactors and/or generators to afford a "nuclear chocolate box" that can be consulted and carefully selected from, depending on the desired application or need.[4]

Indium-111 is an attractive SPECT radionuclide that decays with a half-life of 2.8 days via electron capture (100% EC) and emits two high intensity $\gamma$-rays (245 and 172 keV) with near-ideal energy for diagnostic purposes. This radionuclide is widely available as it is commonly cyclotron-produced via $^{111}Cd$-(p,n)$^{111}In$ and is clinically FDA approved for use in drugs such as Octreoscan ($^{111}In$-pentetreotide), Prostascint ($^{111}In$-capromab), CEA-Scan ($^{111}In$-arcitumonab), MPI indium DTPA In111 (111In- DTPA), and indium In111 oxyquinoline (111In-oxyquinoline).[5] In addition, $^{111}In$ emits Auger electrons that can potentially be used for radiotherapy.[6,7] Lutetium-177 is a reactor-produced therapeutic radiometal ion ($^{176}Lu$(n,$\gamma$)$^{177}Lu$) with a half-life of 6.6 days that emits $\beta^-$ particles, as well as SPECT imageable $\gamma$-rays (113 and 208 keV).[8] Recently, $^{177}Lu$-PSMA therapy has gained popularity as a viable therapeutic option in men with metastatic prostate cancer.[9] Lutetium is a medium-energy $\beta^-$ emitter (490 keV) with a maximal tissue penetration of <2 mm, which provides better irradiation of small tumors.[10] The medicinal application of radiometal nuclides usually requires a bifunctional chelator to bind the radiometal ion in order to form a thermodynamically stable and kinetically inert metal complex, which can then be delivered to the desired site in vivo via an attached targeting vector for imaging or therapy.[11] Besides the clinical relevance of these radionuclides, it is of utmost importance to understand the fundamental coordination chemistry of these metal complexes and the influence of the structural differences on their biological behavior.[12] In terms of the coordination chemistry of $In^{3+}$, owing to its relatively large ionic size of 62−92 pm, it usually attains a coordination number of 7−8 in its complexes.[13] Although hydrated $In^{3+}$ has a high p$K_a$ of 4.0,[14] it is usually considered as a borderline acidic metal ion ($I_A$ = 6.3) with affinity for soft donor groups, such as thiols,[15,16] as well as hard donor groups, such as phenolates and carboxylates.[17,18] While the lanthanide $Lu^{3+}$ is a larger metal ion with an ionic radius of 86−103 pm and

Received: April 9, 2019






DOI: 10.1021/acs.inorgchem.9b01016
Inorg. Chem. XXXX, XXX, XXX−XXX

coordination number 6–9,[13] the metal ion has a strong preference for hard basic donor atoms ($I_A$ = 10.07) such as carboxylates.[19]

Over the past several decades, a plethora of both macrocyclic and nonmacrocyclic chelating ligands have been developed for a variety of radiometal ions.[6,11,14,20,21] Some of these chelators (Chart 1) include DTPA (diethylenetriamine pentaacetic acid), DOTA (1,4,7,10- tetraazacyclododecane-1,4,7,10-tetraacetic acid), $H_4$octapa, $H_4$neunpa, $H_4$octox, and $H_2$bispa$^2$.[10,21–25] DTPA is an FDA-approved $^{111}$In-based radiopharmaceutical that can radiolabel $^{111}In^{3+}$ within 15 min at ambient conditions; however, it is known that DTPA complexes suffer from relatively low kinetic stability, potentially leading to complex degradation and free radiometal release in vivo. Conversely, metal complexes of macrocyclic ligands (e.g., DOTA) generally retain higher thermodynamic stability and kinetic inertness in vivo than the nonmacrocyclic chelators, but typically exhibit slow complexation kinetics. Therefore, they often require radiolabeling at higher temperatures and longer reaction times; a major drawback when working with heat-sensitive antibodies as a targeting vector for the radiopharmaceutical.

**Chart 1. Structures of Ligands Discussed**

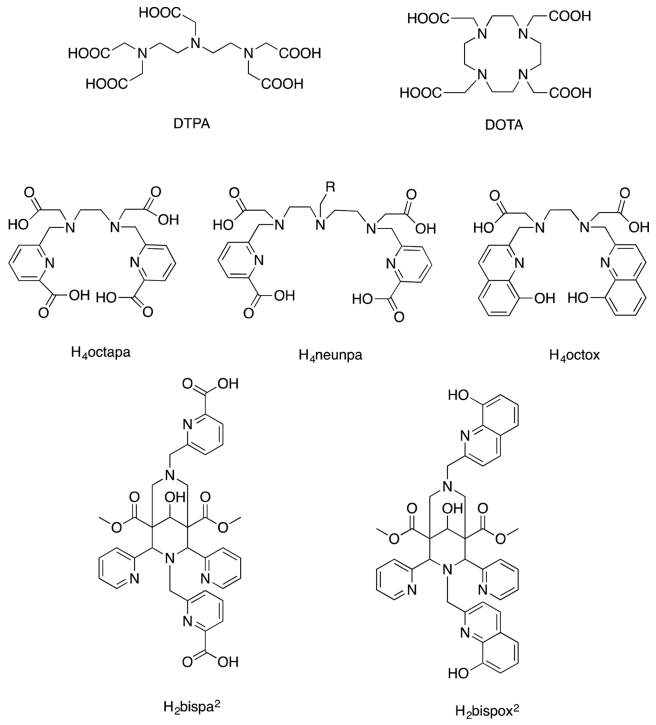


Among the nonmacrocyclic chelators, the recently reported $H_4$octox shows fast chelation with medicinally relevant trivalent metal ions (i.e., $Y^{3+}$, $In^{3+}$, $La^{3+}$, $Lu^{3+}$, and $Gd^{3+}$) and forms very thermodynamically stable complexes in solution.[24] Bispidines are claw-like ligands with a very rigid adamantane-derived backbone, enforcing axial coordination geometries and, depending on the type and number of pendent arms, tetra- up to octadentate ligands with various donor sets have been reported.[25,26] The ensuing reactivities and thermodynamic properties give rise to interesting applications in Fe-based oxidation catalysis,[27] Cu-based aziridination catalysis[28,29] and $^{64/67}$Cu[30–32] as well as $^{111}$In, $^{177}$Lu, and $^{225}$Ac based radiopharmaceutical chemistry.[33] The ligand $H_2$bispa$^2$ consists of the highly preorganized, rigid bispidine backbone, which enforces a particular coordination geometry to the metal ions[34] (a characteristic usually more typical of macrocyclic ligands) and the picolinic acid pendent arms help in faster complexation (characteristic of acyclic chelators).[31,33]

Herein, we report an octadentate chelator, $H_2$bispox$^2$, the design of which was inspired by the $H_2$bispa$^2$ bispidine backbone and $H_4$octox oxinate arms.[24,33,35,36] The complexation behavior

**Scheme 1. Synthesis of $H_2$bispox$^2$, 7**

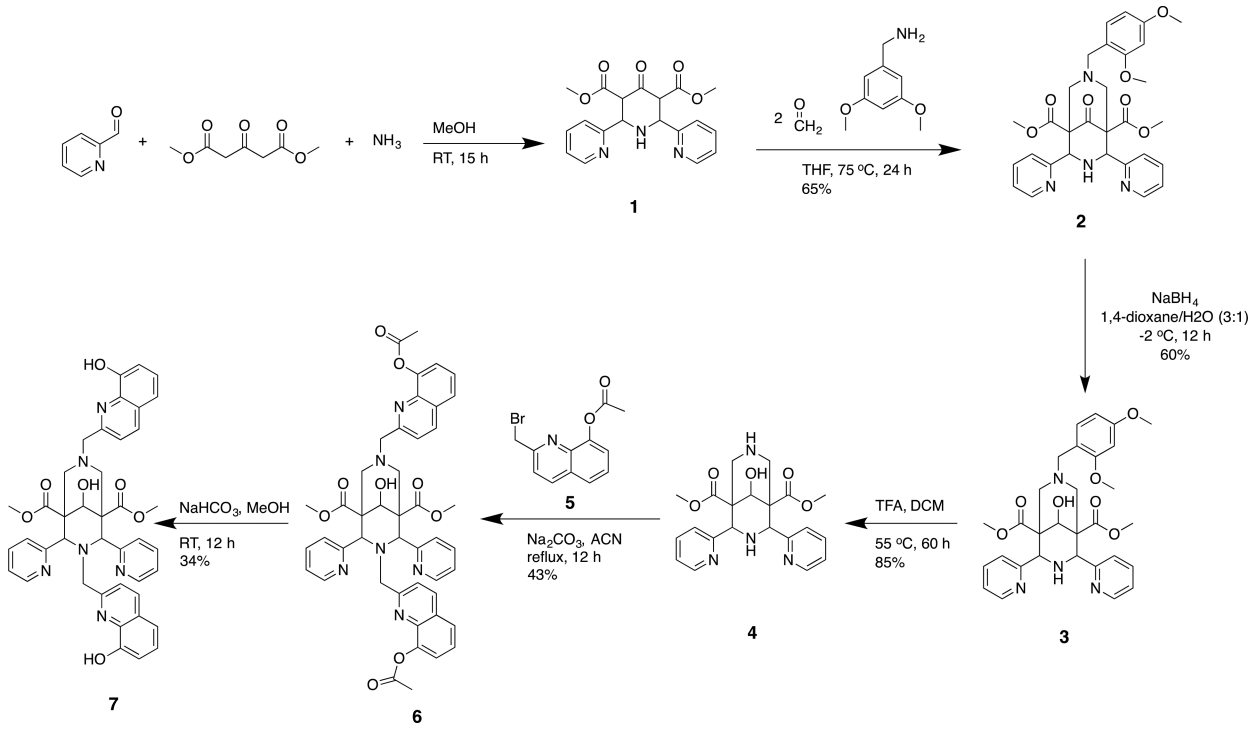




DOI: 10.1021/acs.inorgchem.9b01016
Inorg. Chem. XXXX, XXX, XXX–XXX

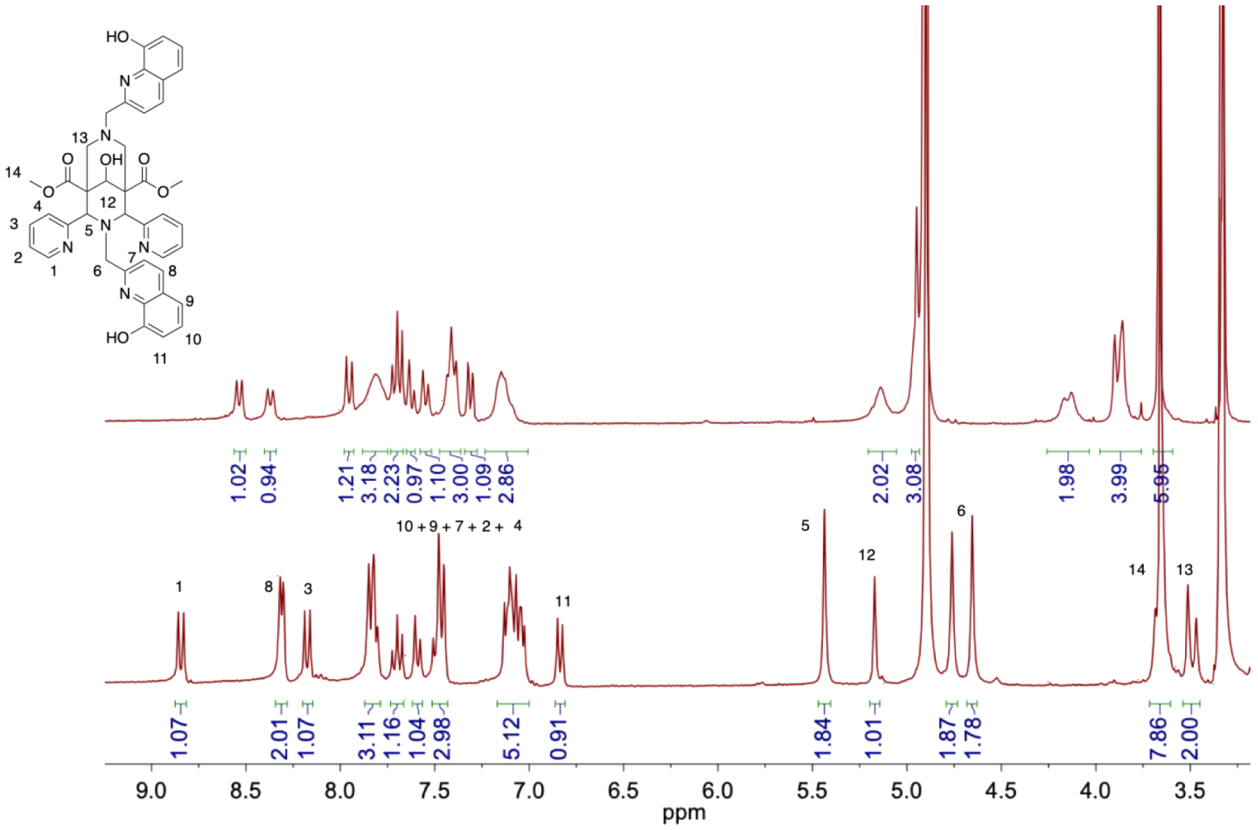


**Figure 1.** $^{1}$H NMR spectra ($CD_3OD$, room temperature, 300 MHz) of $H_2$bispox$^2$ (top) and [In(bispox$^2$)]$^+$ (bottom).

of the $N_6O_2$ donor set ligand, $H_2$bispox$^2$ was investigated with nonradioactive $In^{3+}$ and $Lu^{3+}$ ions and the corresponding binary metal complexes were characterized by nuclear magnetic resonance (NMR) spectroscopy, mass spectrometry (MS), single-crystal X-ray analysis, and infrared spectroscopy (IR). In addition, radiolabeling studies were performed with $^{111}In^{3+}$ and $^{177}Lu^{3+}$ ions. In vitro human serum stability tests with [$^{111}$In(bispox$^2$)]$^+$ were also performed to evaluate the potential application of $H_2$bispox$^2$ as a chelator component in $^{111}$In-based radiopharmaceuticals.

## RESULTS AND DISCUSSION

**Ligand Synthesis and Characterization.** The synthetic route (Scheme 1) for the bispidine-based ligand $H_2$bispox$^2$ [dimethyl 9-hydroxy-3,7-bis((8-hydroxyquinolin-2-yl)methyl)-2,4-di(pyridin-2-yl)-3,7-diazabicyclo[3.3.1]nonane-1,5-dicarboxylate] relies on the bispidol scaffold **4**, which was synthesized via a well-established protocol from commercially available starting materials.[33] The synthesis involves two consecutive Mannich reactions to yield **2** and reduction of the C9 keto group to yield bispidol **3** to prevent a retro-Mannich reaction.[37−39] Deprotection with trifluoroacetic acid led to the intermediate **4**, which was isolated as the trifluoroacetic salt. The alkylating agent 2-(bromomethyl)quinoline-8-yl acetate **5** was synthesized from commercially available 8-hydroxy-2-methylquinoline in two steps via protection of the phenolic −OH as acetate ester, followed by free radical bromination.[40,41] One drawback of using NBS as a brominating agent was its tendency to disubstitute the hydrogens of the methyl group via formation of 2,2′-dibromomethyl-8-hydroxyquinoline. To optimize the reaction conditions NBS and AIBN were added in small aliquots over 4 h reaction time. The alkyl-protected ligand **6** was then synthesized from N-alkylation of the secondary amines of the intermediate **4.** The unreacted side arm **5** was separated from the desired product **6** by eluting through a silica plug with DCM, followed by recrystallization of **6** using EtOAc. Deprotection of the acetate groups of precursor **6** in mildly basic conditions yielded $H_2$bispox$^2$ **7**. The ligand $H_2$bispox$^2$ was characterized by $^{1}$H and $^{13}$C NMR spectroscopy, and low- and high-resolution mass spectrometry.

**Metal Complexes.** The coordination chemistry of the octadentate ligand $H_2$bispox$^2$ with $In^{3+}$ and $Lu^{3+}$ ions was studied for potential application in nuclear medicine. The 1:1 metal complexes were successfully synthesized from equimolar solutions of the ligand and metal salts in methanol. The formation of the metal complexes was confirmed by HR-ESI-MS and ATR-IR as well as $^{1}$H NMR spectroscopy. The $^{1}$H NMR spectrum of [In(bispox$^2$)]$^+$ shows significant changes in the $^{1}$H NMR chemical shifts of both the aromatic (downfield shift) as well as the aliphatic hydrogen atoms of the ligand due to coordination of the ligand to the 3+ cation (Figure 1). In contrast to the corresponding metal complexes of $H_2$bispa$^2$ ($In^{3+}$ and $La^{3+}$) and the [In(octox)]$^-$ complex, there is no splitting of the diasterotopic methylene hydrogen atoms of the five-membered chelate rings involving N3 or N7 and the N atoms of the oxine arm.[24,33] This suggests fluxionality at ambient temperature of the puckered chelate rings of the [bispox$^2$]$^{2-}$ vs the [bispa$^2$]$^{2-}$ complex. We attribute this to less puckering resulting in lower barriers for chelate ring inversion and therefore to more fluxionality, supporting a higher rigidity of the oxine vs the picolinate arms and hence an increase in stability and inertness. Note that other dynamic processes such as changes from 8- to 9-coordination or semidetachment of one of the pyridine donors (as observed in the solid state structures of


DOI: 10.1021/acs.inorgchem.9b01016
Inorg. Chem. XXXX, XXX, XXX−XXX

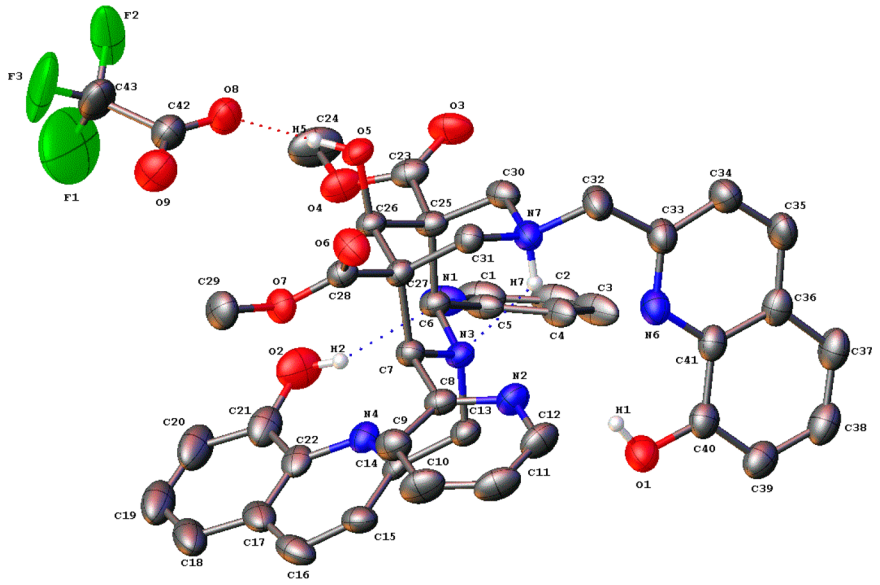


**Figure 2.** ORTEP diagram of $H_2$bispox$^2$. Ellipsoids are shown at the 50% probability level. All hydrogen atoms on carbon atoms are omitted for clarity. The following color code was used: C, gray; H, white; N, blue; O, red; F, green.

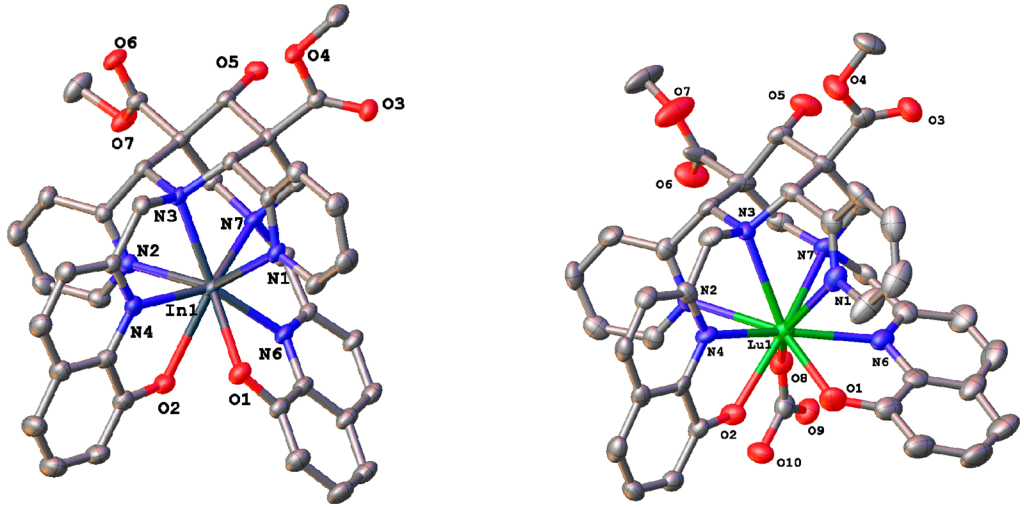


**Figure 3.** ORTEP diagrams of the cation in [In(bispox$^2$)](ClO$_4$) (left) and [Lu(bispox$^2$)(HCO$_3$)] (right). Ellipsoids are shown at the 50% probability level; cocrystallized solvent molecules, counterions, and all hydrogen atoms are omitted for clarity. The following color code was used: C, gray; N, blue; O, red; In, silver; Lu, green.

[In(bispa)$^2$]$^+$, and in bispidine−copper(I) complexes) may also occur but the simple $^1$H NMR spectrum and the relatively sharp lines suggest fast dynamics and a highly symmetrical structure.[33,42] However, the $^1$H NMR spectrum combined with the solid state X-ray analysis confirms the structure and the formation of the metal complex, and it can be concluded that only a single species [In(bispox$^2$)]$^+$ is formed at room temperature in solution as well as in solid state.

**Molecular Structures.** Colorless crystals suitable for single crystal X-ray diffraction were obtained from a saturated solution of the ligand $H_2$bispox$^2$ in methanol that was subjected to diethyl ether diffusion at room temperature. The X-ray diffraction analysis showed that the ligand crystallizes with a TFA anion in a highly preorganized chair−chair conformation, where the pyridine N-donor atoms occupy the favored equatorial position with respect to the six membered azacyclohexane, which is perfectly suitable for metal coordination (Figure 2). Also, one of the rigid 8-hydroxy quinoline moieties in the ligand points toward the metal binding site, which implies that the ligand is partially preorganized (see Supporting Information for detailed experimental structural data).

*X-ray Crystal Structures of Metal Complexes.* Brown colored crystals of [In(bispox$^2$)](ClO$_4$) and orange colored needle-like crystals of [Lu(bispox$^2$)(HCO$_3$)] suitable for solid-state X-ray analysis were obtained by slow diffusion of diethyl ether into a saturated solution of the respective metal complex in MeOH. In the structures shown in Figure 3, In$^{3+}$ is in an eight coordinate environment, with four N-donor atoms from the bispidine backbone and the $N_2O_2$ donor set from the oxine arms, while Lu$^{3+}$ is nine coordinate with an additional O-donor atom from hydrogen carbonate. It is interesting to note that the In−O1 and In−O2 bond lengths are longer than the Lu−O1 and Lu−O2 bond distances (M−O$_{oxine}$, see Table 1). Each structure features a perfect fit of the metal center into the cavity of the ligand.



DOI: 10.1021/acs.inorgchem.9b01016
*Inorg. Chem.* XXXX, XXX, XXX−XXX

Table 1. Selected Bond Distances in [In(bispox$^2$)](ClO$_4$) and [Lu(bispox$^2$)(HCO$_3$)]

| distance [Å] | [In(bispox$^2$)](ClO$_4$) | [Lu(bispox$^2$)(HCO$_3$)] |
|---|---|---|
| M−O1 | 2.511(2) | 2.334(6) |
| M−O2 | 2.565(2) | 2.293(7) |
| M−O8 | NA | 2.254(7) |
| M−N1 | 2.393(2) | 2.607(8) |
| M−N2 | 2.400(2) | 2.627(9) |
| M−N3 | 2.352(2) | 2.711(8) |
| M−N4 | 2.222(2) | 2.459(9) |
| M−N6 | 2.443(2) | 2.704(8) |
| M−N7 | 2.196(2) | 2.456(8) |

It is interesting to compare these two structures with the corresponding In$^{3+}$, Ho$^{3+}$, and Tb$^{3+}$ structures of H$_2$bispa$^2$ (oxine vs picolinate).[33,43] Both ligands lead to structures that are asymmetric with respect to the M−N3/M−N7 (bispidine−N$_{amine}$) distances, as usually observed with the bispidine platform.[44] Interestingly, the two In$^{3+}$ structures are 8- while all others are 9-coordinate. This might be due to the crystallization procedure, specifically in the case of [In(bispa$^2$)]$^+$, where a very unsymmetrical structure is obtained and spectroscopic data suggest that in solution, a solvent molecule is coordinated.[33,43] For the four known structures of the two octadentate bispidine ligands coordinated to Ln$^{3+}$ ions (Tb$^{3+}$, Ho$^{3+}$, and Lu$^{3+}$), the average of the eight bonds to the Ln$^{3+}$ ion is practically identical (2.51−2.53 Å), for In$^{3+}$ these average distances are significantly shorter (2.38, 2.41 Å), although the ionic radius of In$^{3+}$ (0.92 Å, CN 8) is close to that of Lu$^{3+}$ (0.97 Å, CN 8). This may be due to the relatively soft donor sets, which are better suited for In$^{3+}$ than for the lanthanides, and this is supported by the observation that for H$_2$bispox$^2$ the In−O$_{oxine}$ bonds are significantly longer and the In−N bonds shorter than the corresponding bonds for the Lu$^{3+}$ complex (see Table 1). While the average metal-donor bonds are, due to the rigidity of the bispidine cavity, very similar for the complexes with H$_2$bispa$^2$ and H$_2$bispox$^2$ (see above), the distances to the ox arms in general are shorter than the distances to the pa arms, and this may reflect the p$K_a$ values of the corresponding donors (8-hydroxyquinoline; picolinate: 4.94, 9.82; 1.01, 5.39),[45] i.e., the oxine arms are much more basic and may lead to stronger bonds, specifically for softer metal ions (e.g., In$^{3+}$).

**Radiolabeling Experiments.** Initial radiolabeling experiments were done to test the ability of H$_2$bispox$^2$ to radiolabel the SPECT radionuclide $^{111}$In ($t_{1/2}$= 2.8 days) and the theranostic isotope $^{177}$Lu ($t_{1/2}$ = 6.6 days). Quantitative radiolabeling was achieved with $^{111}$InCl$_3$ (57 MBq $\mu$mol$^{-1}$, [L] = 10$^{-5}$ M) at ambient temperature within 15 min, whereas radiolabeling with $^{177}$LuCl$_3$ (60 MBq $\mu$mol$^{-1}$, [L] = 10$^{-5}$ M) required gentle heating at 37 °C for 30 min to achieve quantitative labeling (RCY > 97%). The concentration-dependent radiolabeling was performed at pH 7 and 8 (10 mM NaOAc buffer), respectively and the results are summarized in Table 2. The efficiency of radiolabeling with $^{111}$In$^{3+}$ and $^{177}$Lu$^{3+}$ is very similar to that with the corresponding picolinate ligand H$_2$bispa$^2$ and significantly better than with the "gold standard" DOTA.[33]

Initial radiolabeling studies with the $\alpha$-emitter $^{225}$Ac (~4 MBq $\mu$mol$^{-1}$, [L] = 10$^{-4}$) were attempted with ligand concentrations of 10$^{-4}$ M but unlike milder labeling kinetics with $^{111}$In and $^{177}$Lu, radiolabeling with $^{225}$Ac required heating at 85 °C for 1 h. Due to the inability to quantitatively radiolabel $^{225}$Ac at room temperature, further experiments with $^{225}$Ac were not attempted.

Table 2. Radiochemical Yields (RCY in %) of the Concentration Dependent Experiments for the $^{111}$In−H$_2$bispox$^2$ and $^{177}$Lu−H$_2$bispox$^2$ System

| [ligand] (M) | $^{111}$In RCY (%)[a] | $^{177}$Lu RCY (%)[b] |
|---|---|---|
| 10$^{-4}$ | 99 | 99 |
| 10$^{-5}$ | 95 | 98 |
| 10$^{-6}$ | 71 | 42 |

[a]Room temperature, 10 mM NaOAc, pH = 7, 15 min. [b]37 °C, 10 mM NaOAc, pH = 8, 30 min.

*Human Serum Stability with [$^{111}$In(bispox$^2$)]$^+$.* Human serum contains several endogenous ligands, such as apotransferrin, albumin, and metallothionein that can compete for and displace chelator bound metal ions in vivo. Therefore, it is necessary that any metal−chelate complex must be able to withstand transchelation to such endogenous ligands in order to deliver the radiotracer to the desired molecular target. As a result, the in vivo kinetic inertness of the [$^{111}$In(bispox$^2$)]$^+$ system was estimated by incubating a preformed [$^{111}$In(bispox$^2$)]$^+$ complex in an excess of human serum (37 °C, pH 7.4). Aliquots of each reaction mixture were then removed at 24 h and 5 day time points. The percentage of intact $^{111}$In$^{3+}$ complex was determined by iTLC and was found to be exceptionally high (stable) over 5 days, remaining 89% intact. This stability is comparable to that of [$^{111}$In(bispa$^2$)]$^+$ and exceeds the 5 day stability of [$^{111}$In(octox)]$^-$ (see Table 3).

Table 3. Human Serum Stability Challenge Data Performed at 37 °C ($n$ = 2), with Stability Shown as Percentage of Intact $^{111}$In Complex

| complex | 24 h stability | 5 day stability |
|---|---|---|
| [$^{111}$In(bispox$^2$)]$^+$ | 94.6 ± 0.4 | 89.4 ± 0.6 |
| [$^{111}$In(octox)]$^-$ [a] | 91.4 ± 0.6 | 83.6 ± 1.4 |
| [$^{111}$In(dedpa)]$^+$ [a] | 19.7 ± 1.5 | NA |
| [$^{111}$In(octapa)]$^-$ [a] | 92.3 ± 0.04 | NA |
| [$^{111}$In(DOTA)]$^-$ [a] | 89.4 ± 2.2 | NA |
| [$^{111}$In(DTPA)]$^{2-}$ [a] | 88.3 ± 2.2 | <60 |
| [$^{111}$In(p-NO$_2$−Bn-neunpa)]$^-$ [b] | 97.8 ± 0.1 | 97.8 ± 0.7 |
| [$^{111}$In(bispa$^2$)]$^+$ [c] | 87.4 ± 0.6 | 87.4 ± 1.5 |

[a]Mouse serum stability data performed at ambient temperature; data included from ref 24 for comparison. [b]From ref 46. [c]From ref 33.

These human serum stability results coupled with the mild and efficient radiolabeling protocol suggest that H$_2$bispox$^2$ is a promising chelator for $^{111}$In and $^{177}$Lu pharmaceuticals.

## CONCLUSIONS

In$^{3+}$ and Lu$^{3+}$ complexes of the octadentate oxine-armed bispidine ligand H$_2$bispox$^2$ have, as expected, very similar structural properties as the corresponding complexes of the picolinate-armed bispidine H$_2$bispox$^2$, except that, due to the differences in basicity, the bonds to the oxine arms are stronger than those to the picolinate arms. It is counterintuitive that these ligands have significantly faster complexation kinetics and higher stabilities than other ligands such as the macrocycle-based DOTA and NOTA families—with microscopic reversibility, faster complexation kinetics should lead to faster transchelation. This suggests that the decomplexation mechanism is (slightly) different from the complexation pathway.[25] The efficient


DOI: 10.1021/acs.inorgchem.9b01016
Inorg. Chem. XXXX, XXX, XXX−XXX

radiolabeling at ambient conditions has been suggested to be due to the open cavity of the tetradentate bispidine platform and the planar tridentate N3 or N7-appended picolinate or oxine arms. The stronger bonds to the oxine arms together with the increase in rigidity obviously leads to an improvement with respect to decomplexation. Decomplexation may be induced by protonation of the pendant arms or rather by hydrolysis, i.e., coordination of $OH^-$. Also, it must be noted that compared to $H_2$bispa$^2$, $H_2$bispox$^2$ is more lipophilic and this will have a direct impact on the pharmacokinetics as well as the binding properties. Recently, it has been noted that the increased lipophicility of the chelators leads to the higher tumor uptake and reduced nonspecific binding compared with the hydrophilic chelators.[47,48] Further improvement of these ligands may therefore involve replacement of one of the oxine arms by a tridentate substituent to the bispidine backbone, leading to nonadentate ligands, i.e., preventing a monodentate coligand or solvent molecule from coordinating to the lanthanide center as in the structures observed with $H_2$bispox$^2$. This, together with mechanistic work and in vivo experiments, are now of importance to further develop this area.

## EXPERIMENTAL SECTION

**Materials and Methods.** All solvents and reagents were purchased from commercial suppliers (Sigma-Aldrich, TCI America, Fischer Scientific, Alfa Aesar) and were used as received. Reactions were monitored by TLC (MERCK Kieselgel 60 F254, aluminum sheet). Flash chromatography was performed using Silicaflash F60 silica gel (40−63 $\mu$M particle size), Redisep Rf HP silica columns, and a Combiflash Rf column machine. Water used was ultrapure (18.2 MΩ cm$^{-1}$ at 25 °C, Milli-Q, Millipore, Billerica, MA).

$^1$H and $^{13}$C NMR spectroscopy was performed on either a Bruker Advance 300 or Bruker AV III HD 400 MHz spectrometer. Chemical shifts ($\delta$) are quoted in ppm relative to residual solvent peaks as appropriate. Coupling constants ($J$) are provided in Hertz (Hz). $^1$H NMR signals were designated as follows: s (singlet), d (doublet), t (triplet), q (quartet), quin (quintet), sxt (sextet), spt (septet), m (multiplet), or a combination of these, with br representing a broad signal. Low resolution ESI-MS was performed on a Waters 2965 HPLC-MS with the sample prepared in methanol or ACN. Results are labeled with $m/z$ (abundance percentage) values - $[M+X]^{\mp}$. High resolution ESI-MS was performed on a Waters/Micromass LCT TOF-MS with the sample prepared in methanol. Results are labeled with $m/z$ (abundance percentage) values $-[M + X]^{\mp}$. Semipreparative reverse phase high-performance liquid chromatography (HPLC) for $H_2$bispox$^2$ and [In(bispox$^2$)](ClO$_4$) was performed on a Phenomenex 16 synergi hydro-RP 80 $A°$, 250 × 21.2 mm column connected to a Waters 600 controller, a Waters 2487 dual wavelength absorbance detector, and a Waters delta 600 pump. The HPLC solvents were (A) $H_2O$ containing 0.1% trifluoroacetic acid (TFA) and (B) $CH_3CN$ containing 0.1% TFA.

Silica gel impregnated TLC plates (MERCK Kieselgel 60 F254, aluminum sheet) were used to analyze $^{111}$In and $^{177}$Lu radiolabeling reaction progress and the complex stability, human serum stability tests were counted on a BioScan System 200 imaging scanner equipped with a BioScan Autochanger 1000.

**Synthesis and Characterization.** *Bispidol (**4**).* Compound **4** was prepared according to the literature preparation with appropriate characteristic spectra.[49]

*2-Methylquinolin-8-yl Acetate (**8**).* A solution of 8-hydroxy-2-methylquinoline (5 g, 31.4 mmol) in acetic anhydride (50 mL) was refluxed overnight. The reaction mixture was quenched by the addition of saturated aqueous $NaHCO_3$ (30 mL) and the aqueous layer was extracted with EtOAc (3 × 20 mL). The combined organic layers were dried over anhydrous $Na_2SO_4$ and filtered, and the filtrate was concentrated in vacuo to afford the product as yellow oil (6.32 g, 31.1 mmol, 99%). $^1$H NMR (300 MHz, $CDCl_3$, 25 °C): $\delta$ = 8.04 (d, $J$ = 8.5 Hz, 1H), 7.54 (d, $J$ = 7.6, 1H), 7.46 (m, $J$ = 7.6 Hz, 2H), 7.29 (d, $J$ = 8.5 Hz, 1H), 2.74 (s, 3H), 2.53 (s, 3H). $^{13}$C NMR (75 MHz, $CDCl_3$, 25 °C): $\delta$ = 33.4 (s), 41.6 (s), 122.1 (s), 124.0 (s), 126.7 (s), 126.8 (s), 128.7 (s), 128.8 (s), 134.0 (s), 137.4 (s), 157.3 (s).

*2-(Bromomethyl)quinolin-8-yl Acetate (**5**).* To a solution of 2-methylquinolin-8-yl acetate (4 g, 19.9 mmol, 1.0 equiv) in benzene (40 mL) *N*-bromosuccinimide (1.59 g, 8.94 mmol, 0.45 equiv) was added, followed by addition of AIBN (652 mg, 3.97 mmol, 0.2 equiv). The yellow mixture was refluxed, and after 2 h, second aliquots of NBS (1.59 g, 8.94 mmol, 0.45 equiv) and AIBN (652 mg, 3.97 mmol) were added. After heating for additional 2 h, the reaction mixture was cooled to room temperature, and the solvent was removed under reduced pressure. The residue was dissolved in EtOAc (80 mL) and was washed with saturated aqueous $Na_2S_2O_3$ (200 mL). The aqueous layer was extracted with EtOAc (2 × 80 mL), and the combined organic layers were dried over anhydrous $Na_2SO_4$. The crude product was purified using flash column chromatography (EtOAc/hexane: 25/75) to afford a yellow colored product (3.06 g, 8.01 mmol, 48%). $^1$H NMR (300 MHz, $CDCl_3$, 25 °C): $\delta$ = 8.16 (d, $J$ = 8.5 Hz, 1H), 7.69 (d, $J$ = 8.5 Hz, 1H), 7.59 (d, $J$ = 7.8, 1H), 7.53 (t, $J$ = 7.8 Hz, 1H), 7.46 (d, $J$ = 8.5 Hz, 1H), 4.68 (s, 2H), 2.50 (s, 3H). $^{13}$C NMR (75 MHz, $CDCl_3$, 25 °C): $\delta$ = 169.7 (s), 156.9 (s), 147.4 (s), 140.2 (s), 137.1 (s), 128.5 (s), 126.6 (s), 125.5 (s), 121.8 (s), 121.8 (s), 34.4 (s), 20.9 (s).

*Dimethyl 3,7-Bis((8-acetoxyquinolin-2-yl)methyl)-9-hydroxy-2,4-di(pyridin-2-yl)-3,7-diazabicyclo[3.3.1]nonane-1,5-dicarboxylate (**6**).* To a solution of **4** (450 mg, 1.09 mmol) in dry ACN (20 mL) was added $Na_2CO_3$ (693 mg, 6.54 mmol) and 2-(bromomethyl)quinolin-8-yl acetate (**5**) (610 mg, 2.18 mmol). The reaction mixture was refluxed overnight, filtered to remove $Na_2CO_3$, and concentrated in vacuo. The residue was dissolved in a minimum amount of DCM and poured onto a silica pad and washed several times with EtOAc/hexane (20:80) to remove excess 2-(bromomethyl)quinolin-8-yl acetate followed by a final wash with DCM/MeOH (90:10) to elute the compound. The solvent was evaporated under reduced pressure and the crude product was recrystallized from hot MeOH to afford the product **6** (383 mg, 472 $\mu$mol, 43%). $^1$H NMR (300 MHz, $CDCl_3$, 25 °C): $\delta$ = 8.46 (d, $J$ = 7.9 Hz, 1H), 7.96 (d, $J$ = 7.6 Hz, 2H), 7.74 (t, $J$ = 7.9 Hz, 2H), 7.67 (s br, 1H), 7.63−7.48 (m, 7H), 7.01−6.94 (t, 2H), 6.80 (d, $J$ = 7.2 Hz, 2H), 6.31 (d, $J$ = 8.6 Hz, 1H), 5.68 (s, 2H), 5.09 (s, 1H), 4.87 (s, 2H), 4.58 (d, $J$ = 12.4 Hz, 2H), 4.35 (d, $J$ = 10.2 Hz, 2H), 3.67 (s, 2H), 3.63 (s, 6H), 2.94 (s, 3H), 2.37 (s, 3H). $^{13}$C NMR (75 MHz, $CDCl_3$, 25 °C): $\delta$ = 14.2 (s), 20.9 (s), 21.3 (s), 29.7 (s), 52.7 (s), 60.4 (s), 64.1 (s), 64.7 (s), 67.41 (s), 110.8 (s), 117.9 (s), 119.1 (s), 119.3 (s), 119.8 (s), 121.7 (s), 122.0 (s), 125.6 (s), 125.7 (s), 126.1 (s), 126.3 (s), 127.3 (s), 136.9 (s), 147.5 (s), 151.8 (s), 157.9 (s), 159.3 (s). HR-ESI-MS: $m/z$ calcd for $C_{45}H_{43}N_6O_9^+$ ([M + H]$^+$), 811.3092; found, 811.3096.

*Dimethyl 9-Hydroxy-3,7-bis((8-hydroxyquinolin-2-yl)methyl)-2,4-di(pyridin-2-yl)-3,7-diazabicyclo[3.3.1]nonane-1,5-dicarboxylate, $H_2$bispox$^2$ (**7**).* To a solution of (OAc)$_2$-bispox$^2$ (**6**) (200 mg, 247 $\mu$mol) in MeOH (10 mL) was added saturated aqueous $NaHCO_3$ (5 mL). The reaction mixture was stirred overnight at room temperature. Water was added until a white precipitate formed that was filtered off and carefully washed multiple times with water and diethyl ether. The remaining solid was dried under vacuum and purified by reverse phase (RP)-HLPC using eluents: (A) 0.1% H(TFA) in $H_2O$ and (B) 0.1% TFA in ACN with a linear gradient 40 to 100% B over a period of 35 min and flow rate set to 1 mL/min. The retention time of the ligand was $t_R$ = 9.5 min. The desired fractions were combined and concentrated in vacuo to afford the ligand as yellow solid (61 mg, 83.8 $\mu$mol, 34%). Suitable crystals for X-ray analysis were obtained by slow diffusion of diethyl ether into a solution in MeOH. $^1$H NMR (300 MHz, MeOD, 25 °C): $\delta$ = 8.27 (d, $J$ = 8.6 Hz, 1H), 8.03 (d, $J$ = 8.0 Hz, 1H), 7.83 (m, $J$ = 8.1 Hz, 4H), 7.66 (d, $J$ = 7.7 Hz, 1H), 7.58 (d, $J$ = 8.3 Hz, 1H), 7.50 (t, $J$ = 8.1 Hz, 1H), 7.39 (d, $J$ = 7.0 Hz, 5H), 7.11 (d, $J$ = 7.4 Hz, 1H), 7.03 (m, $J$ = 7.2 Hz, 2H), 6.73 (d, $J$ = 8.4 Hz, 1H), 5.13 (s, 1H), 5.04 (s, 2H), 4.81 (s, 2H), 4.17 (d, $J$ = 13.1 Hz, 2H), 3.96 (s, 2H), 3.77 (d, $J$ = 13.7 Hz, 2H), 3.73 (s, 6H). $^{13}$C NMR (75 MHz, MeOD, 25 °C): $\delta$ = 168.8 (s), 154.6 (s), 152.9 (s), 149.4 (s), 138.4 (s), 137.8 (s), 128.9 (s), 128.1 (s), 125.5 (s), 124.2 (s), 122.7 (s), 121.7 (s), 118.2 (s), 117.8 (s), 114.6 (s), 111.7 (s), 70.7 (s), 70.2 (s), 62.1 (s), 52.9 (s), 52.0 (s), 49.5 (s). HR-ESI-MS: $m/z$ calcd for $C_{41}H_{38}KN_6O_7^+$ ([M+K]$^+$), 765.2439;


DOI: 10.1021/acs.inorgchem.9b01016
Inorg. Chem. XXXX, XXX, XXX−XXX

found, 765.2438. IR (KBr pellet): $\tilde{\nu}$ [$cm^{-1}$] = 3060 w, 2958 w, 1734 m, 1678 s, 1593 m, 1572 m, 1512 m, 1463 m, 1438 m, 1255 m, 1199 vs, 1174 vs, 1129 vs, 1093 s, 949 m, 833 m, 801 s, 752 s, 720 vs.

*[In(bispox$^2$)](ClO$_4$).* To a solution of $H_2$bispox$^2$ (15 mg, 20.6 μmol, 1.0 equiv) in MeOH (5 mL) was added a solution of $In(ClO_4)_3 \cdot 8H_2O$ (11.5 mg, 20.6 μmol, 1.0 equiv) in MeOH (5 mL), the pH of the solution was adjusted to pH ∼ 8 using 0.1 M NaOH, and the resultant yellow colored solution was stirred at room temperature for 5 h. The solvent was concentrated in vacuo, the crude solid was purified by reverse phase (RP)-HPLC using eluents: (A) 0.1% TFA in $H_2O$ and (B) ACN with a linear gradient 5 to 100% B over a period of 35 min and flow rate set to 1 mL/min. The retention time of the metal complex was $t_R$ = 15.25 min. The desired fractions were combined and concentrated in vacuo to yield orange colored product (7.64 mg, 8.13 μmol, 39%). Suitable crystals for X-ray analysis were obtained by slow evaporation of a solution in MeOH. $^1$H NMR (300 MHz, MeOD, 25 °C): $\delta$ = 8.84 (d, $J$ = 8.5 Hz, 1H), 8.31 (d, $J$ = 4.8 Hz, 2H), 8.17 (d, $J$ = 8.5 Hz, 1H), 7.87−7.78 (m, 3H), 7.70 (t, $J$ = 8.0 Hz, 1H), 7.59 (d, $J$ = 8.1 Hz, 1H), 7.51−7.45 (m, 3H), 7.15−7.01 (m, 5H), 6.84 (d, $J$ = 7.8 Hz, 1H), 5.44 (s, 2H), 5.17 (s, 1H), 4.76 (s, 2H), 4.65 (s, 2H), 3.68−3.66 (m, 8H), 3.49 (d, $J$ = 13.3 Hz, 2H). $^{13}$C NMR (75 MHz, MeOD, 25 °C): $\delta$ = 168.9 (s), 152.1 (s), 149.5 (s), 142.9 (s), 141.1 (s), 140.4 (s), 130.7 (s), 130.5 (s), 130.3 (s), 129.1 (s), 125.7 (s), 125.3 (s), 120.9 (s), 119.0 (s), 114.1 (s), 113.9 (s), 71.7 (s), 70.5 (s), 63.7 (s), 54.4 (s), 52.2 (s), 51.5 (s). HR-ESI-MS, (pos, MeOH): [$In^{III}$(bispox$^2$)]$^+$ calcd for $C_{41}H_{36}InN_6O_7$ [M]$^+$, 837.1686; found, 837.1677. IR (KBr pellet): $\tilde{\nu}$ [$cm^{-1}$] = 2953 m, 2924 m, 2854 m, 1733 m, 1606 m, 1507 w, 1466 m, 1441 m, 1276 m, 1255 m, 1089 vs, 1054 vs, 959 m, 836 m, 755 s.

*Radiolabeling.* A stock solution of $H_2$bispox$^2$ was made (1.3 mg/mL, ∼$10^{-3}$ M) in 1:1 ACN/DI water. Using serial dilution, ligand solutions with concentrations of $10^{-4}$- $10^{-6}$ M were prepared by addition of pH 7 NaOAc (10 mM) buffer in screw-cap mass spectrometry vials such that the total volume per reaction was 500 μL after the addition of $^{111}InCl_3$ or $^{177}LuCl_3$. An aliquot of $^{111}InCl_3$ or $^{177}LuCl_3$ (∼100−300 kBq) was added to the vials containing the ligand and buffer, and allowed to react (radiolabel) at ambient temperature for 15 min for $^{111}$In or was heated at 37 °C for 30 min for $^{177}$Lu radiolabeling. The reaction mixture was analyzed by spotting a small aliquot on aluminum-backed silica TLC plated developed in mobile phase: 10 mM EDTA solution (pH = 7). With EDTA as mobile phase, uncomplexed $^{111}$In or $^{177}$Lu migrates up the plate as EDTA complex ($R_f$ > 0.5) while [$^{111}$In(bispox$^2$)]$^-$ or [$^{177}$Lu(bispox$^2$)]$^-$ species stay on the baseline ($R_f$ = 0). Developed plates were counted immediately and the radiolabeling yields were calculated by integrating the peaks in the radio-chromatogram, which is consistent with the well-separated radiopeaks of the free metal and the complex on the HPLC radiotraces ($t_R$ = 4.8 min for "free" $^{111}$In and 12.8 min for [$^{111}$In(bispox)]$^+$ complex.

*$^{111}$In Complex Stability Studies in Human Serum.* The compound [$^{111}$In(bispox$^2$)]$^-$ was prepared with radiolabeling procedure as described above. To the reaction vial containing the radiometal-chelate complex (500 μL), an equal volume of human serum was added and the competition mixture was incubated at 37 °C. At time points 1 day and 5 days, aliquots were spotted on aluminum-backed silica TLC plates and developed with 10 mM EDTA solution (pH = 7) as mobile phase.

*Solid State X-ray Analysis.* Single colorless rectangular-shaped crystals of $H_2$bispox$^2$ were recrystallized from a methanol/diethyl ether mixture by slow evaporation. A suitable crystal (0.47 × 0.31 × 0.36 mm$^3$) was selected and mounted on a Mylar loop with oil on a Bruker APEX II area detector diffractometer. The crystal was kept at $T$ = 100(2) K during data collection. Using Olex2,[50] the structure was solved with the XT[51] structure solution program, using the Intrinsic Phasing solution method. The model was refined with version 2017/1 of XL[51] using least squares minimization.

Single yellow rectangular-shaped crystals of [In(bispox$^2$)](ClO$_4$) were recrystallized from methanol by slow evaporation. A suitable crystal (0.20 × 0.13 × 0.11 mm$^3$) was selected and mounted on a Mylar loop with oil on a Bruker APEX II area detector diffractometer. The crystal was kept at $T$ = 100(2) K during data collection. Using Olex2,[50] the structure was solved with the XT[51] structure solution program, using the intrinsic phasing solution method. The model was refined with version 2017/1 of XL[51] using least squares minimization.

Single orange rectangular-shaped crystals of [Lu(bispox$^2$)($HCO_3$)] were obtained by recrystallization from methanol solution. A suitable crystal (0.16 × 0.12 × 0.06 mm$^3$) was selected and mounted on a suitable support on an Bruker APEX-II CCD diffractometer. The crystal was kept at a steady $T$ = 98(2) K during data collection. The structure was solved with the SIR2004[52] structure solution program by using the direct methods solution method and by using Olex2[50] as the graphical interface. The model was refined with version 2018/1 of ShelXL[53] using least squares minimization.

## ■ ASSOCIATED CONTENT

### Supporting Information

The Supporting Information is available free of charge on the ACS Publications website at DOI: 10.1021/acs.inorgchem.9b01016.

Detailed information on $^1$H NMR and $^{13}$C NMR spectra of compounds, FT-IR spectra, X-ray crystallography data (including tables of bond lengths and angles), and detailed i-TLC radiochromatographs (PDF)

### Accession Codes

CCDC 1908810−1908812 contain the supplementary crystallographic data for this paper. These data can be obtained free of charge via www.ccdc.cam.ac.uk/data_request/cif, or by emailing data_request@ccdc.cam.ac.uk, or by contacting The Cambridge Crystallographic Data Centre, 12 Union Road, Cambridge CB2 1EZ, UK; fax: +44 1223 336033.

## ■ AUTHOR INFORMATION


### Corresponding Authors

*(C.O.) E-mail: orvig@chem.ubc.ca.

*(P.C.) E-mail: Peter.Comba@aci.uni-heidelberg.de.

### ORCID

Xiaozhu Wang: 0000-0002-5882-0066

Peter Comba: 0000-0001-7796-3532

Chris Orvig: 0000-0002-2830-5493


### Notes

The authors declare no competing financial interest.

## ■ ACKNOWLEDGMENTS

We gratefully acknowledge both the Canadian Institutes for Health Research (CIHR) and the Natural Sciences and Engineering Research Council (NSERC) for grant support, NSERC for an IsoSiM CREATE at TRIUMF studentship (N.C.) and for CGS M and PGS D scholarships (L.S.) as well as MITACS for a Globalink Graduate fellowship (N.C.) and UBC for a FYF (L.S.). P.C. acknowledges support by the Deutsche Forschungsgemeinschaft (DFG) and Heidelberg University. TRIUMF receives funding from the National Research Council of Canada. We also thank Mr. Thomas Kostelnik for thoughtful editing.

## ■ REFERENCES

(1) Blumgart, H. L.; Yens, O. C. Studies on the Velocity Of Blood Flow I. The Method Utilized. *J. Clin. Invest.* **1927**, *4*, 1−13.

(2) Blumgart, H. L.; Yens, O. C. Studies on the Velocity Of Blood Flow. *Ann. Int. Med.* **1976**, *84*, 747.

(3) Hoehr, C.; Bénard, F.; Buckley, K.; Crawford, J.; Gottberg, A.; Hanemaayer, V.; Kunz, P.; Ladouceur, K.; Radchenko, V.; Ramogida, C.; Robertson, A.; Ruth, T.; Zacchia, N.; Zeisler, S.; Schaffer, P. Medical isotope production at TRIUMF- from imaging to treatment. *Phys. Procedia* **2017**, *90*, 200−208.



DOI: 10.1021/acs.inorgchem.9b01016
*Inorg. Chem.* XXXX, XXX, XXX−XXX

(4) Blower, P. J. A nuclear chocolate box: the periodic table of nuclear medicine. *Dalton Trans.* **2015**, *44*, 4819−4844.
(5) Cyclotron Produced Radionuclides. *Physical Characteristics and Production Methods*; An International Atomic Energy Agency Publication: Vienna, 2009.
(6) Kostelnik, T. I.; Orvig, C. Radioactive Main Group and Rare Earth Metals for Imaging and Therapy. *Chem. Rev.* **2019**, *119*, 902−956.
(7) Kersemans, V.; Cornelissen, B.; Minden, M. D.; Brandwein, J.; Reilly, R. M. Drug-Resistant AML Cells and Primary AML Specimens Are Killed by 111In-Anti-CD33 Monoclonal Antibodies Modified with Nuclear Localizing Peptide Sequences. *J. Nucl. Med.* **2008**, *49*, 1546−1554.
(8) Holland, J. P.; Williamson, M. J.; Lewis, J. S. Unconventional nuclides for radiopharmaceuticals. *Mol. Imaging* **2010**, *9*, 1−20.
(9) Emmett, L.; Willowson, K.; Violet, J.; Shin, J.; Blanksby, A.; Lee, J. Lutetium $^{177}$ PSMA radionuclide therapy for men with prostate cancer: a review of the current literature and discussion of practical aspects of therapy. *J. Med. Radiat. Sci.* **2017**, *64*, 52−60.
(10) Banerjee, S.; Pillai, M. R. A.; Knapp, F. F. Lutetium-177 Therapeutic Radiopharmaceuticals: Linking Chemistry, Radiochemistry, and Practical Applications. *Chem. Rev.* **2015**, *115*, 2934−2974.
(11) Price, E. W.; Orvig, C. Matching chelators to radiometals for radiopharmaceuticals. *Chem. Soc. Rev.* **2014**, *43*, 260−290.
(12) Heppeler, A.; Froidevaux, S.; Mäcke, H. R.; Hennig, M.; Jermann, E.; Béhé, M.; Powell, P. Radiometal-Labelled Macrocyclic Chelator-Derivatised Somatostatin Analogue with Superb Tumour-Targeting Properties and Potential for Receptor-Mediated Internal Radiotherapy. *Chem. - Eur. J.* **1999**, *5*, 1974−1981.
(13) Shannon, R. D. Revised Effective Ionic Radii and Systematic Studies of Interatomie Distances in Halides and Chaleogenides. *Acta Crystallogr., Sect. A: Cryst. Phys., Diffr., Theor. Gen. Crystallogr.* **1976**, *A32*, 751−767.
(14) Wadas, T. J.; Wong, E. H.; Weisman, G. R.; Anderson, C. J. Coordinating Radiometals of Copper, Gallium, Indium, Yttrium and Zirconium for PET and SPECT Imaging of Disease. *Chem. Rev.* **2010**, *110*, 2858−2902.
(15) Sun, Y.; Anderson, C. J.; Pajeau, T. S.; Reichert, D. E.; Hancock, R. D.; Motekaitis, R. J.; Martell, A. E.; Welch, M. J. Indium(III) and Gallium(III) Complexes of Bis(aminoethanethiol) Ligands with Different Denticities: Stabilities, Molecular Modeling, and in Vivo Behavior. *J. Med. Chem.* **1996**, *39*, 458−470.
(16) Briand, G. G.; Cooper, B. F. T.; MacDonald, D. B. S.; Martin, C. D.; Schatte, G. Preferred bonding motif for indium aminoethanethiolate complexes: structural characterization of (Me2NCH2CH2S)-2InX/SR (X = Cl, I; R = 4-MeC6H4, 4-MeOC6H4). *Inorg. Chem.* **2006**, *45*, 8423−8429.
(17) Hunt, F. C. Potential Radiopharmaceuticals for the Diagnosis of Biliary Atresia and Neonatal Hepatitis: EHPG and HBED Chelates of 67Ga and 111In. *Int. J. Radiat. Appl. Instrumentation. Part B. Nucl. Med. Biol.* **1988**, *15*, 659−664.
(18) Price, E. W.; Ferreira, C. L.; Adam, M. J.; Orvig, C. High-denticity Ligands Based on Picolinic Acid for 111In Radiochemistry. *Can. J. Chem.* **2014**, *92*, 695−705.
(19) Stimmel, J. B.; Kull, F. C. Samarium-153 and Lutetium-177 Chelation Properties of Selected Macrocyclic and Acyclic Ligands. *Nucl. Med. Biol.* **1998**, *25*, 117−125.
(20) Mjos, K. D.; Orvig, C. Metallodrugs in Medicinal Inorganic Chemistry. *Chem. Rev.* **2014**, *114*, 4540−4563.
(21) Boros, E.; Packard, A. B. Radioactive Transition Metals for Imaging and Therapy. *Chem. Rev.* **2019**, *119*, 870−901.
(22) Price, E. W.; Zeglis, B. M.; Cawthray, J. F.; Ramogida, C. F.; Ramos, N.; Lewis, J. S.; Adam, M. J.; Orvig, C. H4octapa-Trastuzumab: Versatile Acyclic Chelate System for 111In and 177Lu Imaging and Therapy. *J. Am. Chem. Soc.* **2013**, *135*, 12707−12721.
(23) Ferdani, R.; Stigers, D. J.; Fiamengo, A. L.; Wei, L.; Li, B. T. Y.; Golen, J. A.; Rheingold, A. L.; Weisman, G. R.; Wong, E. H.; Anderson, C. J. Synthesis, Cu(II) complexation, 64Cu-labeling and biological evaluation of cross-bridged cyclam chelators with phosphonate pendant arms. *Dalton Trans.* **2012**, *41*, 1938−1950.
(24) Wang, X.; Jaraquemada-Peláez, M. de G.; Rodríguez-Rodríguez, C.; Cao, Y.; Buchwalder, C.; Choudhary, N.; Jermilova, U.; Ramogida, C. F.; Saatchi, K.; Häfeli, U. O.; Patrick, B. O.; Orvig, C. H4octox: Versatile Bimodal Octadentate Acyclic Chelating Ligand for Medicinal Inorganic Chemistry. *J. Am. Chem. Soc.* **2018**, *140*, 15487−15500.
(25) Comba, P.; Kerscher, M.; Rück, K.; Starke, M. Bispidines for radiopharmaceuticals. *Dalton Trans.* **2018**, *47*, 9202−9220.
(26) Comba, P.; Kerscher, M.; Schiek, W. Bispidine coordination chemistry. *Prog. Inorg. Chem.* **2008**, *55*, 613.
(27) Comba, P.; Fukuzumi, S.; Koke, C.; Martin, B.; Löhr, A.-M.; Straub, J. A bispidine iron(IV) oxo complex in the entatic state. *Angew. Chem., Int. Ed.* **2016**, *55*, 11129−11133.
(28) Comba, P.; Merz, M.; Pritzkow, H. Catalytic Aziridination of Styrene with Copper Complexes of Substituted 3,7-Diazabicyclo[3.3.1]nonanones. *Eur. J. Inorg. Chem.* **2003**, *9*, 1711−1718.
(29) Comba, P.; Haaf, C.; Lienke, A.; Muruganantham, A.; Wadepohl, H. Synthesis, Structure, and Highly Efficient Copper-Catalyzed Aziridination with a Tetraaza-Bispidine Ligand. *Chem. - Eur. J.* **2009**, *15*, 10880−10887.
(30) Roux, A.; Nonat, A. M.; Brandel, J.; Hubscher-Bruder, V.; Charbonnière, L. J. Kinetically Inert Bispidol-Based Cu(II) Chelate for Potential Application to $^{64/67}$ Cu Nuclear Medicine and Diagnosis. *Inorg. Chem.* **2015**, *54*, 4431−4444.
(31) Comba, P.; Grimm, L.; Orvig, C.; Rück, K.; Wadepohl, H. Synthesis and Coordination Chemistry of Hexadentate Picolinic Acid Based Bispidine Ligands. *Inorg. Chem.* **2016**, *55*, 12531−12543.
(32) Juran, S.; Walther, M.; Stephan, H.; Bergmann, R.; Steinbach, J.; Kraus, W.; Emmerling, F.; Comba, P. Hexadentate Bispidine Derivatives as Versatile Bifunctional Chelate Agents for Copper(II) Radioisotopes. *Bioconjugate Chem.* **2009**, *20*, 347−359.
(33) Comba, P.; Jermilova, U.; Orvig, C.; Patrick, B. O.; Ramogida, C. F.; Rück, K.; Schneider, C.; Starke, M. Octadentate Picolinic Acid-Based Bispidine Ligand for Radiometal Ions. *Chem. - Eur. J.* **2017**, *23*, 15945−15956.
(34) Comba, P.; Lienke, A. Bispidine Copper(II) Compounds: Effects of the Rigid Ligand Backbone Peter. *Inorg. Chem.* **2001**, *40*, 5206−5209.
(35) Imbert, D.; Comby, S.; Chauvin, A.-S.; Bünzli, J.-C. G. Lanthanide 8-Hydroxyquinoline-Based Podates with Efficient Emission in the NIR Range. *Chem. Commun.* **2005**, *11*, 1432−1434.
(36) Mouralian, C.; Buss, J. L.; Stranix, B.; Chin, J.; Ponka, P. Mobilization of Iron from Cells by Hydroxyquinoline-Based Chelators. *Biochem. Pharmacol.* **2005**, *71*, 214−222.
(37) Comba, P.; Jakob, M.; Kerscher, M. The tetradentate bispidine ligand 3,7-dimethyl-9-oxo-2,4-bis(2-pyridyl)-3,7-diazabicyclo[3.3.1]-nonane-1,5-dicarboxylate methylester, and its copper(II) complex. *Inorg. Synth.* **2010**, *35*, 70−73.
(38) Samhammer, A.; Holzgrabe, U.; Haller, R. Synthese, Stereochemie Und Analgetische Wirkung von 3,7-Diazabicyclo[3.3.1]nonan-9-Onen Und 1,3-Diazaadamantan-6-onen[1]). *Arch. Pharm.* **1989**, *322*, 551−555.
(39) Comba, P.; Kanellakopulos, B.; Katsichtis, C.; Lienke, A.; Pritzkow, H.; Rominger, F. Synthesis and Characterisation of manganese(II) Compounds with Tetradentate Ligands Based on the Bispidine Backbone. *J. Chem. Soc., Dalton Trans.* **1998**, 3997−4002.
(40) Serdyuk, O. V.; Evseenko, I. V.; Dushenko, G. A.; Revinskii, Y. V.; Mikhailov, I. E. Synthesis, Structure, and Luminescent Properties of 2-[2-(9-Anthryl)vinyl]quinolines. *Russ. J. Org. Chem.* **2012**, *48*, 78−82.
(41) Walkup, G. K.; Imperiali, B. Stereoselective Synthesis of Fluorescent $\alpha$-Amino Acids Containing Oxine (8-Hydroxyquinoline) and Their Peptide Incorporation in Chemosensors for Divalent Zinc. *J. Org. Chem.* **1998**, *63*, 6727−6731.
(42) Börzel, H.; Comba, P.; Hagen, K. S.; Katsichtis, C.; Pritzkow, H. A copper(I) oxygenation precursor in the entatic state: Two isomers of a copper(I) compound of a rigid tetradentate ligand. *Chem. - Eur. J.* **2000**, *6*, 914−919.


DOI: 10.1021/acs.inorgchem.9b01016
*Inorg. Chem.* XXXX, XXX, XXX−XXX

(43) Braun, F.; Comba, P.; Grimm, L.; Herten, D.-P.; Pokrandt, B.; Wadepohl, H. Ligand-sensitized lanthanide(III) luminescence with octadentate bispidines. *Inorg. Chim. Acta* **2019**, *484*, 464−468.
(44) Comba, P.; Kerscher, M.; Merz, M.; Müller, V.; Pritzkow, H.; Remenyi, R.; Schiek, W.; Xiong, Y. Structural Variation in Transition-Metal Bispidine Compounds. *Chem. - Eur. J.* **2002**, *8*, 5750−5760.
(45) Martell, A. E.; Smith, R. M.; Motekaitis, R. J. *NIST Database 46*; National Institute of Standards and Technology: Gaithersburg, MD, 2001.
(46) Spreckelmeyer, S.; Ramogida, C. F.; Rousseau, J.; Colpo, N.; Jermilova, U.; Dias, G. M.; Dude, I.; Jaraquemada-Pelaéz, M. d. G.; Benard, F.; Schaffer, P.; Orvig, C.; et al. p-NO2−Bn−H4neunpa and H4neunpa−Trastuzumab: Bifunctional Chelator for Radiometalpharmaceuticals and 111In Immuno-Single Photon Emission Computed Tomography Imaging. *Bioconjugate Chem.* **2017**, *28*, 2145−2159.
(47) Eder, M.; Schäfer, M.; Bauder-Wüst, U.; Hull, W.-E.; Wängler, C.; Mier, W.; Haberkorn, U.; Eisenhut, M. 68Ga-complex lipophilicity and the targeting property of a urea-based PSMA inhibitor for PET imaging. *Bioconjugate Chem.* **2012**, *23*, 688−697.
(48) Sarkar, S.; Bhatt, N.; Ha, Y. S.; Huynh, P. T.; Soni, N.; Lee, W.; Lee, Y. J.; Kim, J. Y.; Pandya, D. N.; An, G. Il; Lee, K. C.; Chang, Y.; Yoo, J. High in Vivo Stability of Cu-64-Labeled Cross-Bridged Chelators Is a Crucial Factor in Improved Tumor Imaging of RGD Peptide Conjugates. *J. Med. Chem.* **2018**, *61*, 385−395.
(49) Comba, P.; Jakob, M.; Rück, K.; Wadepohl, H. Tuning of the properties of a picolinic acid-based bispidine ligand for stable copper(II) complexation. *Inorg. Chim. Acta* **2018**, *481*, 98−105.
(50) Dolomanov, O. V.; Bourhis, L. J.; Gildea, R. J.; Howard, J. A. K.; Puschmann, H. OLEX2: a complete structure solution, refinement and analysis program. *J. Appl. Crystallogr.* **2009**, *42*, 339−341.
(51) Sheldrick, G. M. Crystal structure refinement with SHELXL. *Acta Crystallogr., Sect. C: Struct. Chem.* **2015**, *C71*, 3−8.
(52) Burla, M. C.; Caliandro, R.; Camalli, M.; Carrozzini, B.; Cascarano, G. L.; Giacovazzo, C.; Mallamo, M.; Mazzone, A.; Polidori, G.; Spagna, R. SIR2011: a new package for crystal structure determination and refinement. *J. Appl. Crystallogr.* **2012**, *45*, 357−361.
(53) Spek, A. L. PLATON SQUEEZE: a tool for the calculation of the disordered solvent contribution to the calculated structure factors. *Acta Crystallogr., Sect. C: Struct. Chem.* **2015**, *C71*, 9−18.



DOI: 10.1021/acs.inorgchem.9b01016
*Inorg. Chem.* XXXX, XXX, XXX−XXX